


 Cite this: *RSC Adv.*, 2021, **11**, 4237

# Decontamination of dense nonaqueous-phase liquids in groundwater using pump-and-treat and *in situ* chemical oxidation processes: a field test

 Tian Xie,<sup>ab</sup> Zhi Dang,<sup>a</sup> Jian Zhang,<sup>c</sup> Qian Zhang,<sup>b</sup> Rong-Hai Zhang,<sup>bd</sup> Chang-Jun Liao<sup>b</sup> and Gui-Ning Lu<sup>\*a</sup>

Groundwater remediation is difficult because of the complexity of the treatment area and the presence of various pollutants, and it is difficult to achieve using a single process. A combined pump-and-treat (P&T) and *in situ* chemical oxidation (ISCO) system was used to remove dense nonaqueous-phase liquids (DNAPLs) from groundwater at the field scale in this study. The underground water pH, electrical conductivity, dissolved oxygen concentration, and  $\text{SO}_4^{2-}$  concentration were used as indirect evidence of *in situ* chemical reactions. Groundwater remediation using the P&T-ISCO process using 1.5% sodium persulfate and 0.03% sodium hydroxide had a remarkable effect on DNAPLs, and the DNAPL diffusion distance was much higher under pumping conditions than under natural conditions. During groundwater remediation, the pollutant concentration positively correlated with the pH, electrical conductivity, and dissolved oxygen concentration and negatively correlated with the  $\text{SO}_4^{2-}$  concentration. In summary, P&T-ISCO can effectively accelerate DNAPL degradation to give efficient groundwater remediation.

Received 26th November 2020

Accepted 12th January 2021

DOI: 10.1039/d0ra10010b

[rsc.li/rsc-advances](http://rsc.li/rsc-advances)

## 1. Introduction

Groundwater contamination with non-aqueous phase liquids and dense non-aqueous phase liquids (DNAPLs) poses one of the most difficult remediation challenges in the environmental engineering field.<sup>1</sup> Water extraction occurs at almost all groundwater decontamination sites. Pump-and-treat (P&T) remediation often initially decreases the contaminant concentration in the extracted water, but then the concentration decreases only gradually over decades.<sup>2</sup> Conventional P&T processes have a poor record in remediating DNAPL-contaminated aquifers because of the low water solubilities and aqueous diffusivities of DNAPLs.<sup>3</sup> The hydrogeological characteristics of a field site (the electrical conductivity (EC), well performance, and contamination distribution) are critical to the performance of a P&T system.<sup>4</sup> Cleaning up DNAPLs using P&T processes is challenging because DNAPLs tend to remain as a residue held in place by capillary pressure.<sup>1</sup> Long plume tailing (back-diffusion) can release persistent pollutants

through molecular diffusion after the primary source of contamination has been decreased.<sup>5</sup>

Surfactant-enhanced remediation has been used to accelerate the solubilization and mobilization of DNAPLs during P&T processes.<sup>6</sup> *In situ* bioremediation using a surfactant foam has been successfully used to mobilize and disperse trichloroethene (TCE), and a bioaugmentation technique was used to remediate the TCE *in situ*.<sup>7</sup> Complete biological dechlorination of chlorinated compounds such as TCE, *cis*-1,2-dichloroethene, and vinyl chloride (VC) to achieve clean-up objectives takes years.<sup>8</sup> The less-permeable zone continues to act as a source of groundwater contamination during the post-bioremediation phase.

*In situ* chemical oxidation (ISCO) is a remediation technique that was developed to clean up contaminated soil and groundwater *in situ*. Chemical oxidation is a quicker groundwater decontamination technique than bioremediation. Contaminated solids and groundwater have been remediated *in situ* using Fenton reagents,<sup>9</sup> potassium permanganate,<sup>10,11</sup> and persulfate.<sup>12</sup> Pollutant degradation during short oxidation periods has been assessed in many laboratory and pilot-scale studies.<sup>9,13,14</sup> However, few long-term studies of DNAPL remediation have been conducted.

Remediation using a P&T process has been combined with an advanced oxidation process to remove DNAPLs (*e.g.*, TCE) in a post-extraction (aboveground) step.<sup>15</sup> Oxidants such as persulfate used in ISCO have long-term slow oxidation effects on groundwater pollutants.<sup>16</sup> This could help control back-diffusion after the expected oxidation period has ended. Persulfate has a half-life of weeks–months underground and is a promising oxidant for use in ISCO.<sup>17,18</sup> Activated persulfate is a novel ISCO oxidant that has been

<sup>a</sup>Institute of Environment and Energy, South China University of Technology, Guangzhou 510006, PR China. E-mail: GNLU@foxmail.com

<sup>b</sup>National Technology Center, Guangxi Bossco Environmental Protection Technology Co Ltd, Nanning 530004, China

<sup>c</sup>Institute of Light Industry and Food Engineering, Guangxi University, Nanning 53004, PR China

<sup>d</sup>College of Environmental Science and Engineering, Guilin University of Technology, Guilin 541006, PR China



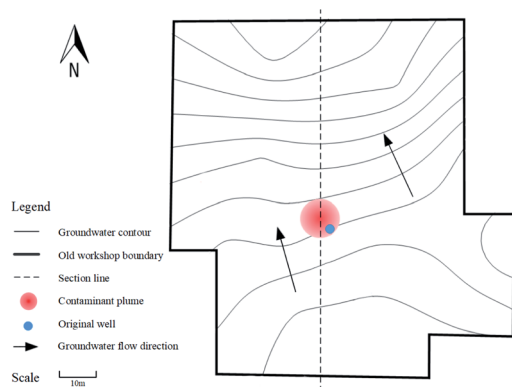


Fig. 1 Schematic diagram of the pollution plane.

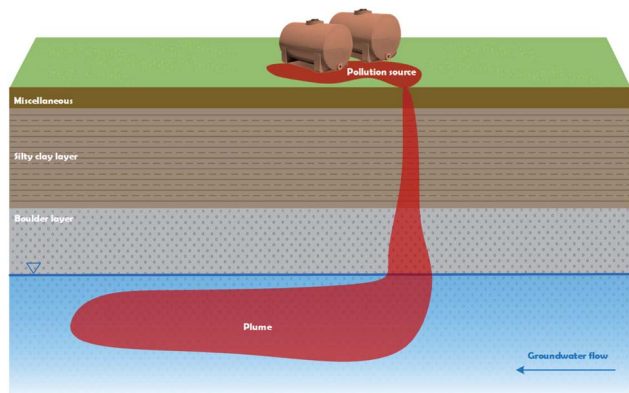
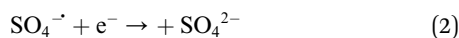


Fig. 2 Schematic diagram of the pollution profile.

combined with activation methods such as heating, adding transition metals ions, and creating alkaline conditions.<sup>19</sup> The equations for persulfate activation are shown in eqn (1) and (2).<sup>20</sup> Factors such as the pH, oxidation–reduction potential, and EC have been used to predict the mobilities, distributions, and reactivities of ISCO oxidants in the field.<sup>21</sup>



Five types of DNAPL pollutants were continually monitored at a test site during a P&T process for four months. The pollutant concentrations in the monitoring wells fluctuated soon after the P&T system was shut down, making it possible to determine the effect of the ISCO-enhanced P&T process at the pilot scale on back-diffusion of DNAPL pollutants.

The objective of this field-scale study was to evaluate the feasibility of using a P&T-ISCO process using sodium persulfate oxidation to remediate groundwater contaminated with DNAPL pollutants using sodium hydroxide as an alkaline agent.<sup>22</sup> Indirect markers (the pH, EC, dissolved oxygen (DO) concentration, and  $\text{SO}_4^{2-}$  concentration) were monitored, and a hydraulic dispersion simulation was performed to accurately evaluate the mobility and reactivity of persulfate in the field.

## 2. Materials and methods

### 2.1 Field site

The test site was at a demolished chemical industrial complex in southern China. Improper disposal of chlorinated organic solvents and solid waste at the site over the past few decades has resulted in point-source pollution, and there are large amounts of DNAPLs in the aquifer. A small-scale point pollution plume of five types of DNAPL was remediated in this study.

The pollution plume is shown schematically in Fig. 1 and 2. The pollution plume was in the middle of an old workshop, and the strata were, from top to bottom, miscellaneous, sill clay, boulders, and mudstone. The groundwater generally flows from southeast to northwest. The profile along the dashed line in Fig. 1 is shown in Fig. 2. Geological drilling and hydrogeological survey data indicated that the water level was 16.5 m below the surface, the aquifer was 20 m thick, the permeability coefficient was  $1.0 \times 10^{-2} \text{ cm s}^{-1}$ , and the hydraulic gradient was 0.002. The VC, 1,1-dichloroethane (1,1-DCA), 1,2-dichloroethane (1,2-DCA), 1,1,2-trichloroethane (1,1,2-TCA), and TCE concentrations in original well were 3350, 59 120, 965, 917, and 320  $\mu\text{g L}^{-1}$ , respectively. The well was seriously polluted and had good hydraulic connections, which was very useful for this study. Some wells for sampling monitoring would be set around it, and monitoring indicators included the pH, EC, DO,  $\text{SO}_4^{2-}$  concentration, and the five pollutions concentration.

Table 1 Pump-and-treat and *in situ* chemical oxidation treatment phases

| Phase | Implementation content   |
|-------|--|
| I     | DNAPL pollutants were restored by P&T Technology, and the concentration of which was continuously monitored. Only when the level of contaminants tended to be stable could the extraction treatment be stopped   |
| II    | DNAPL pollutants were restored by P&T-ISCO Technology, the extraction treatment and <i>in situ</i> chemical oxidation injection were carried out simultaneously. The pollutant concentration, water quality parameters, and chemical diffusion were continuously monitored. After the pollutant concentration reached the target value and tended to be stable, the extraction treatment was stopped |
| III   | The concentration of pollutants and $\text{SO}_4^{2-}$ were monitored continuously until the level of pollutants remained stable for 90 days   |



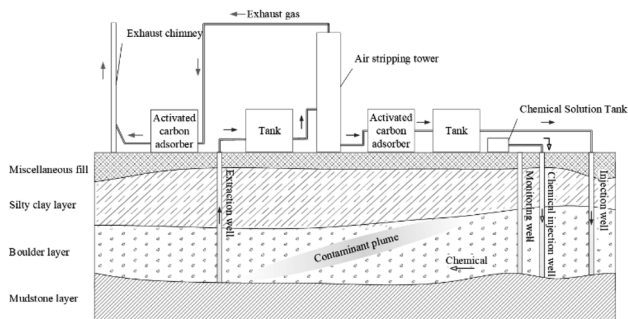


Fig. 3 Pump-and-treat and *in situ* chemical oxidation treatment process.

## 2.2 Methods

Various pollutants can be efficiently and cheaply degraded simultaneously using P&T techniques. ISCO can effectively remove refractory pollutants, but it is expensive to treat large plumes. Therefore, combining P&T and ISCO could be efficient and relatively cheap.

(1) **Test phase.** The P&T technique was used as the main treatment, and the ISCO technique was used to supplement the treatment and to complete the treatment of refractory pollutants. The groundwater remediation field test using the P&T-ISCO technique was divided into three phases, shown in Table 1 and Fig. 3.

(2) **Test parameters.** Before the field test was performed, groundwater samples were collected and analyzed to determine parameters relevant to the P&T-ISCO technique. The parameters used in the subsequent tests are shown in Table 2.

(3) **Test layout.** The original well, marked in Fig. 1, was used as the chemical injection well, and an extraction well, reinjection

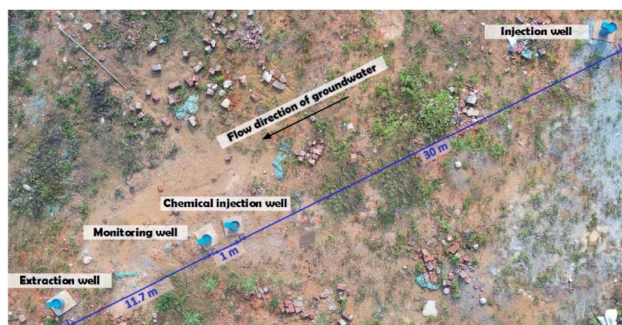


Fig. 4 Locations of the wells used in the pump-and-treat and *in situ* chemical oxidation treatment tests.

well, and monitoring well were situated upstream and downstream, as shown in Fig. 4. A canvas water storage tank and a chemical solution tank are shown in Fig. 5 and 6, respectively.

(4) **Sampling.** The testing process involved sampling and analysis. The sampling and analysis requirements and parameters for each stage are shown in Table 3. And the sampling method was in accordance with Chinese environmental protection industry standard.<sup>24</sup>

Parameters including the pH, DO concentration, and EC were measured using an Orion Star A329 multi-meter (Thermo Fisher Scientific, Waltham, MA, USA) and flow-through cells. TCE and the DCAs were extracted by liquid-liquid extraction using hexane and were quantified using an Agilent 7890 gas chromatograph (Agilent Technologies, Santa Clara, CA, USA) equipped with an electron capture detector. Gas-phase compounds such as acetylene, ethane, ethylene, and VC were

Table 2 Pump-and-treat and *in situ* chemical oxidation treatment parameters<sup>a</sup>

| Name                       | Parameter  |
|----------------------------|--|
| Extraction well            | The diameter was 250 mm and the flow was set as 60 m <sup>3</sup> d <sup>-1</sup>  |
| tank                       | Two tanks of 70 m <sup>3</sup> were set  |
| Air stripping tower        | Two stripping tower with a diameter of 1.8 m and a height of 5 m were set, equipped with roots fans with a charge of 3 kW and an air volume of 4.23 m <sup>3</sup> min <sup>-1</sup> . The gas water ratio was 100, hydraulic retention time was 120 min, and temperature was 25 °C  |
| Activated carbon adsorbers | Two activated carbon adsorbers for wastewater with a diameter of 1 m and a height of 1.3 m were set, and the diameter and height of the activated carbon adsorber for waste gas were 1 m and 1.25 m, respectively. The coal-based activated carbon should be controlled by the following factors: the specific surface area was greater than 900 m <sup>2</sup> g <sup>-1</sup> , the adsorption rate of CCl <sub>4</sub> was greater than 50%, the iodine value was more significant than 900 mg g <sup>-1</sup> , and the loading density distribution was in the range of 550–500 g L <sup>-1</sup> |
| Injection well             | The diameter was 250 mm and the reinjection flow was consistent with the extraction flow, which was set as 60 m <sup>3</sup> d <sup>-1</sup>   |
| Chemical injection well    | The diameter was 200 mm and the injection flow rate was regulated to meet the needs of simultaneous injection and no overflow  |
| Chemical solution tank     | Two chemical solution tanks of 10 m <sup>3</sup> were set. 222.70 m <sup>3</sup> of 1.5% sodium persulfate solution and 0.05% sodium hydroxide would be injected into the injection well   |
| Monitoring well            | The diameter was 250 mm  |

<sup>a</sup> The chemical demand was calculated using the Freundlich linear isothermal adsorption formula.<sup>23</sup>





Fig. 5 Canvas water storage tank.



Fig. 6 Chemical solution tank.

determined by placing liquid samples in headspace vials and allowing gas–liquid equilibrium to be reached, then analyzing the headspace gases using a gas chromatograph equipped with a flame ionization detector. The sulfate concentrations were determined using a Dionex ICS-5000 ion chromatograph (Thermo Fisher Scientific).

### 3. Results and discussion

#### 3.1 DNAPL removal

(1) **Phase I: P&T.** Groundwater was treated using the P&T process from the 1st to the 120th day. It can be seen from Table 4

and Fig. 7 that the ESMs for all five pollutants had decreased after 120 d of the P&T process and that the 1,1-DCA, TCE, and VC concentrations had reached the target values (the maximum concentration of each pollutant defined by the technical guidelines<sup>25</sup> and the class IV of standard for groundwater quality<sup>26</sup>). P&T can therefore effectively remediate various DNAPLs simultaneously.

The 1,2-DCA, TCE, and VC concentrations reached the target values on the 60th day. The 1,1-DCA and 1,1,2-TCA concentrations had decreased by 21.5% and 71.9%, respectively, but the ESMs were still high (22.48 and 9.29, respectively). The initial VC and 1,2-DCA concentrations were relatively low, and the target value was easily reached. The boiling point of VC is  $-13.8\text{ }^{\circ}\text{C}$ , so VC could readily be separated as a gas from the liquid phase at the stripping temperature of  $25\text{ }^{\circ}\text{C}$ .

The P&T process was unable to bring the 1,1-DCA and 1,1,2-TCA concentrations to the target values by the 120th day, and the ESMs at that point were 1.53 and 3.30, respectively. The 1,1-DCA concentration decreased at a markedly higher rate than the 1,1,2-TCA concentration. The high initial concentration meant that the 1,1-DCA and 1,1,2-TCA removal rates were proportional to the Henry's law coefficients (0.0059 and 0.0012, respectively).<sup>27–29</sup> This meant that 1,1-DCA was separated from the water more efficiently than 1,1,2-TCA.

The P&T process was stopped from the 120th to the 180th day. The concentrations of the five pollutants increased and became stable, and the 1,2-DCA, TCE, and VC concentrations (which had reached the target values) remained below the target values. Increasing pollutant concentrations after treatment stops is a common phenomenon in P&T processes.<sup>30</sup> This is because the aquifer will contain large amounts of pebbles, coarse sand, and loose sediment with large specific surface areas<sup>31,32</sup> and adsorption and desorption strongly affects the removal of pollutants at high concentrations.<sup>33</sup> It was therefore particularly important to perform follow-up processing and ISCO.

(2) **Phase II: P&T-ISCO.** In this phase, ISCO was performed as the P&T process continued. Pre-pumping was performed from the 180th to the 182nd days, and sodium hydroxide and sodium persulfate solutions were injected into the injection well on the 200th and 202nd days, respectively.

The test well was well connected to the aquifer, so the pollutant concentrations were stable from the 180th to the 200th days and were not affected by the two-day pre-pump episodes.

Table 3 Sampling and analysis requirements and parameters<sup>a</sup>

| Detection index                                       | Purpose  | Sampling time: buried depth (frequency)   |
|---|--|---|
| Concentration of VC, 1,1-DCA, 1,2-DCA, 1,1,2-TCA, TCE | Analyse the changing trend of pollutants                                   | Phase I: 27 m (every 15 days)<br>Phase II: 27 m (every two days)<br>Phase III: 27 m (every 15 days) |
| pH, DO, EC  | Analyse the change of water quality parameters with injection              | Phase II: 19, 22, 25, 27 m (every 2 days)   |
| Concentration of $\text{Na}_2\text{S}_2\text{O}_8$    | Reflect the diffusion of $\text{Na}_2\text{S}_2\text{O}_8$ after injection | After $\text{Na}_2\text{S}_2\text{O}_8$ injection: 27 m (every 2 hours)                             |
| Concentration of $\text{SO}_4^{2-}$                   | Analyse whether there was secondary pollution                              | Phase II: 19, 22, 25, 27 m (every 2 days)<br>Phase III: 19, 22, 25, 27 m (every 15 days)            |

<sup>a</sup> Analysis of water from the original well indicated that the vertical pollutant distribution was uneven and the highest pollutant concentrations were at 27 m deep.



Table 4 Dense nonaqueous-phase liquid concentrations in the test well

| Name      | Target value<br>( $\mu\text{g L}^{-1}$ ) | Time (d) |        |     |     |      |     |     |     |     |     |
|-----------|--|----------|--------|-----|-----|------|-----|-----|-----|-----|-----|
|           |  | 0        | 60     | 105 | 120 | 180  | 204 | 208 | 224 | 228 | 318 |
| VC        | 90                                       | 3350     | 60     | 65  | 66  | 73   | 58  | 57  | 60  | 56  | 61  |
| 1,1-DCA   | 565                                      | 59 122   | 12 701 | 915 | 864 | 1187 | 712 | 396 | 390 | 362 | 379 |
| 1,2-DCA   | 147                                      | 964      | 141    | 116 | 104 | 107  | 101 | 97  | 93  | 100 | 94  |
| 1,1,2-TCA | 71                                       | 917      | 660    | 248 | 234 | 405  | 182 | 276 | 47  | 45  | 48  |
| TCE       | 300                                      | 321      | 213    | 237 | 222 | 225  | 210 | 189 | 204 | 201 | 186 |

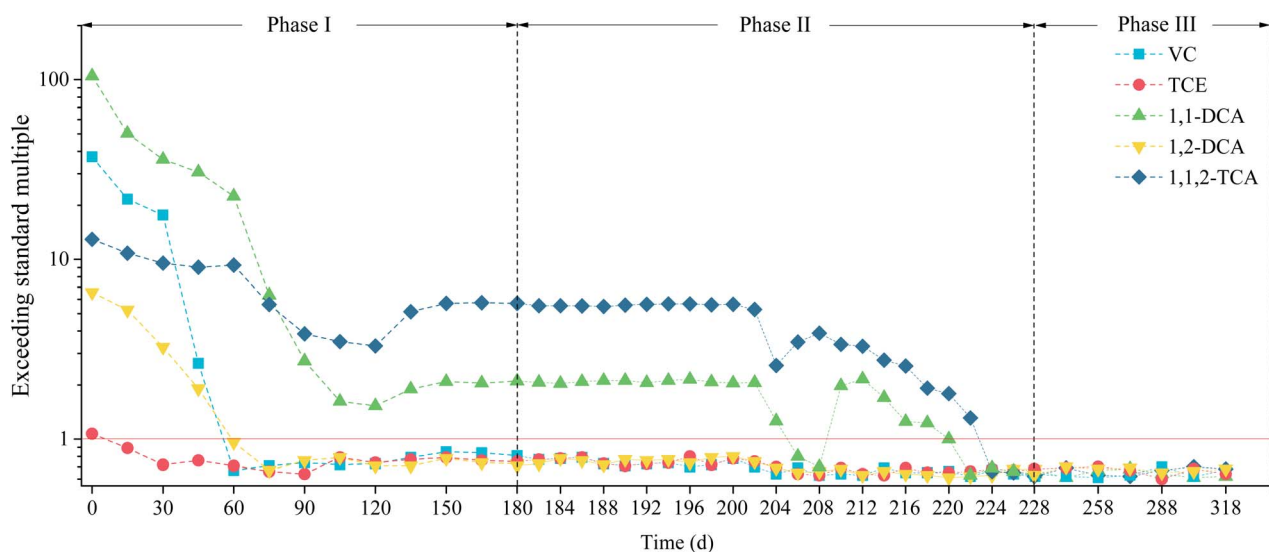


Fig. 7 Dense nonaqueous-phase liquid concentrations exceeding the relevant standards during the 318 d operating period.

Large amounts of pharmaceuticals entered the aquifer between the 202nd and 210th days, and the pollutant concentrations in the groundwater decreased sharply. Convection and diffusion then caused the pollutants gradually to become uniformly distributed throughout the groundwater environment.

After the 212nd day, the 1,1-DCA and 1,1,2-TCA curves both followed downward trends. The 1,1-DCA and 1,1,2-TCA ESMS were 2.16 and 3.29, respectively, but the 1,1-DCA concentration was much higher than the 1,1,2-TCA concentration, and 1,1-DCA reached the target value earlier than 1,1,2-TCA. The pollutant concentration fell below the target value by the 224th day.

**(3) Phase III: follow-up monitoring.** The 1,1-DCA, 1,2-DCA, 1,1,2-TCA, TCE, and VC concentrations fluctuated slightly (by 9.37%, 2.21%, 10.32%, 2.26%, and 12.10%, respectively) and did not exceed the target values.

The concentrations of the five pollutants fluctuated over time during the remediation process. This would have been because the density of all five DNAPLs was greater than water and would have been unevenly distributed in the aquifer.<sup>34,35</sup> It would also have been caused by transformations between halogenated organic compounds.<sup>36–38</sup> These factors would have caused small changes in the pollutant concentrations.

The results described above indicated that the P&T process directly affected various DNAPLs. The P&T process brought the concentrations of three pollutants down to meet the target values in 120 d. The 1,1,2-TCA and 1,1-DCA ESMS had decreased by 78.5% and 28.6%, respectively, by the 120th day. The ISCO process combined with the P&T process was very efficient and appropriate, and the 1,1,2-TCA and 1,1-DCA concentrations reached the target values within 22 d of the oxidant being added. In summary, to use the P&T-ISCO process, the phase I duration should be set according to the difficulty of degrading the pollutants present. In particular, the phase I period should be prolonged as appropriate when there are many pollutants and the pollutant concentrations are much higher than the target values. The amount of oxidant added should be increased when the pollutant concentrations increase in phase II to ensure that the pollutants are effectively degraded.

### 3.2 Water quality parameters

In phase II, the effect of  $\text{Na}_2\text{S}_2\text{O}_8$  activated by NaOH on the removal of pollutants was affected by the groundwater environment.<sup>39</sup> The pH, DO concentration, and EC were monitored at different depths, and the results are shown in Fig. 8–10.



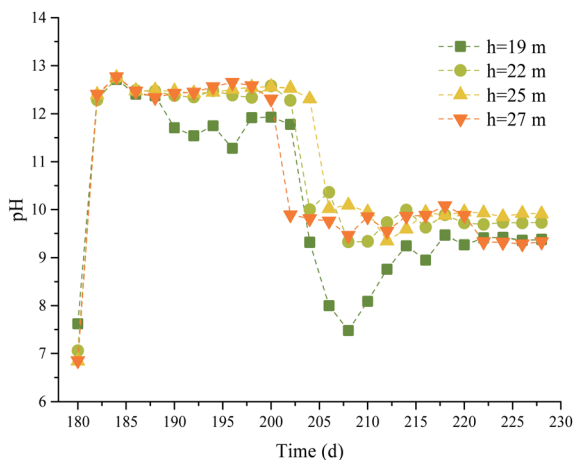


Fig. 8 pH values at different depths between days 180 and 228.

It can be seen from the figures that the groundwater at different depths in the test well before the chemical was injected had pH values of 6.85–7.62, ECs of 326–1293  $\mu\text{S cm}^{-1}$ , and DO concentrations of 2.98–6.26  $\text{mg L}^{-1}$ . After 0.05% NaOH was added to the test well, the pH of the groundwater in the test well increased, reaching a maximum of pH 12.65 at 27 m deep. The ECs also increased sharply, and the maximum ECs at 19, 22, 25, and 27 m deep were  $9.20 \times 10^3$ ,  $1.31 \times 10^5$ ,  $1.34 \times 10^5$ , and  $1.36 \times 10^5 \mu\text{S cm}^{-1}$ , respectively. The DO concentrations fluctuated. After 1.5%  $\text{Na}_2\text{S}_2\text{O}_8$  was added to the test well, the pH values first decreased and then became stable in the range pH 9.33–9.93. The ECs fluctuated and became stable after 206 d. The ECs on the 222nd day at 19, 22, 25, and 27 m deep were 734, 11 640, 14 840, and 12 500  $\mu\text{S cm}^{-1}$ , respectively. The DO concentrations decreased over time, and the concentrations at 19, 22, 25, and 27 m deep were 57.7%, 57.1%, 35.9%, and 53.6% lower, respectively, than before the  $\text{Na}_2\text{S}_2\text{O}_8$  was added.

Correlations between the parameters and the ESMs for 1,1-DCA and 1,1,2-TCA were assessed using SPSS software (IBM, Armonk, NY, USA). The Pearson correlation coefficients are shown in Table 5. For 1,1-DCA, the EC positively correlated with

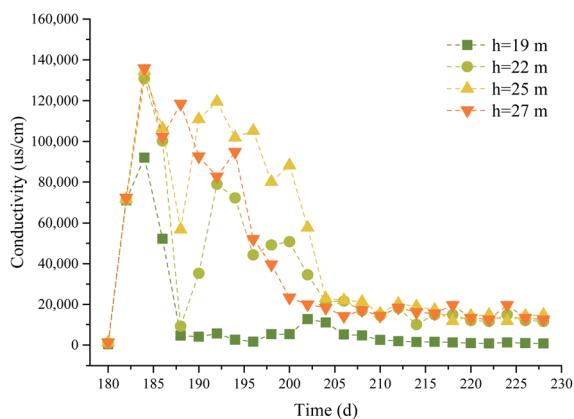


Fig. 9 Electrical conductivities at different depths between days 180 and 228.

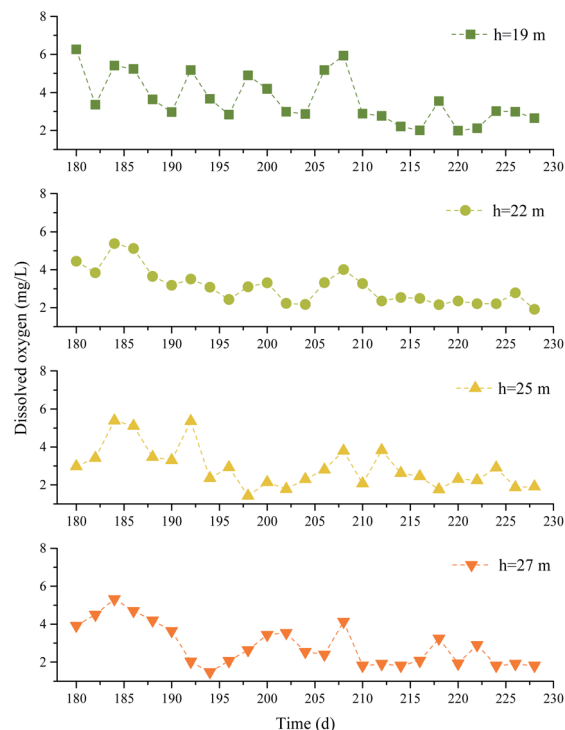


Fig. 10 Dissolved oxygen concentrations between days 180 and 228.

the ESM. For 1,1,2-TCA, the EC extremely positively correlated with the ESM. For 1,1,2-TCA, the pH and DO concentration positively correlated with the ESM.

The groundwater pH directly affected the chemical oxidant reactivity, the DO concentration determined the activity and activation ability of the water and gases, and the EC correlated strongly with the ion concentrations.<sup>40,41</sup> The pollutant concentrations decreased as the pollutants reacted with  $\text{Na}_2\text{S}_2\text{O}_8$ , and the free energy at the interface of the chemical system and the diffusion capacity decreased, so the EC and DO concentration in the groundwater became less variable. The pH, EC, and DO concentration eventually became stable when the  $\text{Na}_2\text{S}_2\text{O}_8$  was consumed and the reaction was completed because of groundwater excretion and recharge. In summary, the pH, EC, and DO concentration were closely related to the ESMs of the pollutants.

### 3.3 Hydraulic dispersion

Migration of  $\text{S}_2\text{O}_8^{2-}$  in the aquifer was simplified to a two-dimensional dispersion problem in a one-dimensional stable flow field<sup>42</sup> and the analytical expression of the  $\text{S}_2\text{O}_8^{2-}$  concentration in the observation well at  $(x_0, y_0)$  could be written

$$C_0 = \frac{M}{4\pi n u t \sqrt{\alpha_L \alpha_T}} \exp \left[ -\frac{(x_0 - ut)^2}{4\alpha_L ut} - \frac{y_0^2}{4\alpha_T ut} - \lambda t \right], \quad (3)$$

where  $C_0$  is the  $\text{S}_2\text{O}_8^{2-}$  concentration at time  $t$  at  $(x_0, y_0)$ ,  $M$  is the instantaneous  $\text{S}_2\text{O}_8^{2-}$  mass at the unit aquifer thickness,  $n$  is the effective porosity of the aquifer,  $u$  is the groundwater flow rate,  $\alpha_L$  and  $\alpha_T$  are the vertical and horizontal dispersion



**Table 5** Pearson correlation coefficients for the pH, electrical conductivity (EC), and dissolved oxygen concentration (DO)<sup>a</sup>

| Parameter | 1,1-DCA | 1,1,2-TCA |
|-----------|---------|-----------|
| pH        | 0.36    | 0.467*    |
| EC        | 0.447*  | 0.556**   |
| DO        | 0.23    | 0.496*    |

<sup>a</sup> \*\* means that the correlation coefficient was significant at the 1% level, \* means that the correlation coefficient was significant at the 5% level.

degrees of the aquifer, respectively, and  $\lambda$  is the  $S_2O_8^{2-}$  attenuation coefficient.

The  $S_2O_8^{2-}$  concentrations at (0,0) and (1,0) were determined. The data were processed using eqn (3), and a curve was fitted to give the parameters  $\alpha_L$ ,  $\alpha_T$ ,  $u$ , and  $\lambda$ . The  $M$  value was  $3768 \text{ mg m}^{-1}$ ,  $n$  was 0.37, and  $\alpha_L$ ,  $\alpha_T$ ,  $u$ , and  $\lambda$  were 0.17 m, 0.035  $\text{m h}^{-1}$ , 0.009, and 0.02 m, respectively. The relationships between the  $S_2O_8^{2-}$  concentration and time in the chemical injection well and the observation well are shown in Fig. 11.

These parameters were processed using eqn (3), and the  $S_2O_8^{2-}$  diffusion distances under pumping and natural conditions are shown in Table 6. The relationship between the  $S_2O_8^{2-}$  concentration and  $x_0$  is shown in Fig. 12.

It can be seen from Fig. 12 that the maximum  $S_2O_8^{2-}$  concentration decreased as time increased and the  $S_2O_8^{2-}$  concentration decreased markedly as the diffusion distance increased. After 24 h, the maximum concentration was <20% of the initial concentration. The  $S_2O_8^{2-}$  consumption rate in the groundwater was therefore very high and should have been sufficient for  $S_2O_8^{2-}$  injection to cause effective diffusion and ensure remediation. It can be seen from Table 6 that the  $S_2O_8^{2-}$  diffusion distances under pumping and natural conditions were 1.17–5.45 and 0.20–1.33 m, respectively. In other words, the diffusion distance was 3.1–5 times higher under pumping conditions than natural conditions and the  $S_2O_8^{2-}$  diffusion distance was much

**Table 6**  $S_2O_8^{2-}$  diffusion distances under different conditions

| Time (h) | The diffusion distance (m)                         |   |
|----------|--|---|
|          | Pumping condition ( $u = 0.035 \text{ m h}^{-1}$ ) | Natural condition ( $u = 0.0041 \text{ m h}^{-1}$ ) |
| 6        | 1.17   | 0.20  |
| 12       | 1.85   | 0.40  |
| 24       | 2.92   | 0.70  |
| 36       | 3.83   | 0.93  |
| 48       | 4.67   | 1.14  |
| 60       | 5.45   | 1.33  |

higher at the pumping velocity than at the natural speed. ISCO was therefore enhanced by increasing the flow rate.

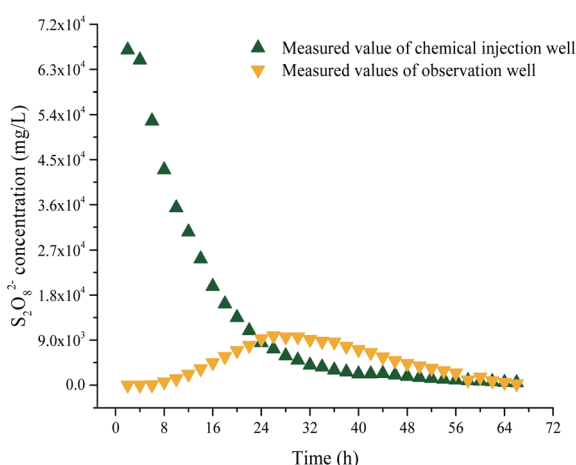
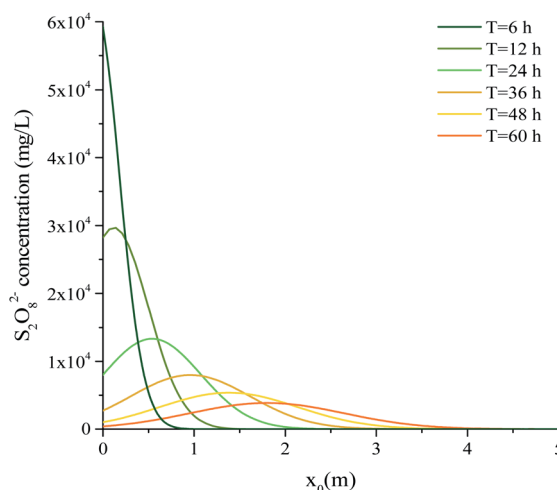
In practice, ISCO often requires large investments of time and money.<sup>43,44</sup> Slow chemical diffusion also causes high chemical concentrations in the local groundwater-soil environment. As mentioned above, the P&T-ISCO process could cause a fast and stable groundwater flow field to form and could increase the migration speeds of chemicals through hydraulic drive. This would cause the distances chemicals would diffuse and the effective scope to increase, meaning the groundwater remediation efficiency would be considerable.

The P&T-ISCO process gave a higher remediation efficiency and shorter remediation time than the ISCO process. The advantages of the ISCO process were retained and the side effects were weakened, so the P&T-ISCO process was much more efficient than the ISCO process.

### 3.4 $SO_4^{2-}$ variations

The P&T-ISCO process strongly positively affected groundwater remediation, but the high  $SO_4^{2-}$  concentration remaining in the groundwater after remediation meant that temporal variations in the  $SO_4^{2-}$  concentrations needed to be assessed.

It can be seen from Fig. 13 that, from the 200th to the 204th days, the  $SO_4^{2-}$  concentration increased almost linearly after

**Fig. 11**  $S_2O_8^{2-}$  concentrations between days 0 and 68.**Fig. 12**  $S_2O_8^{2-}$  concentration plotted against diffusion distance.

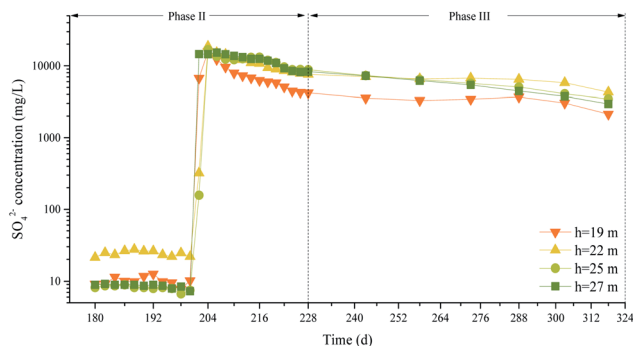


Fig. 13  $\text{SO}_4^{2-}$  concentrations at different depths between days 180 and 318.

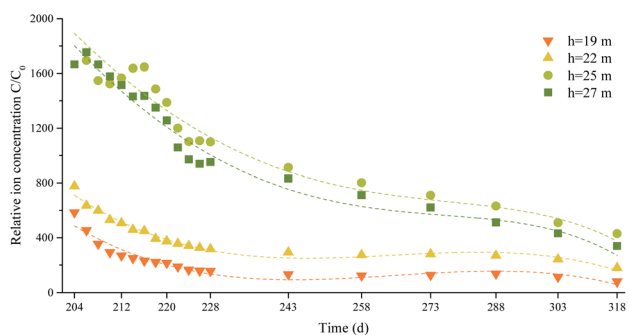


Fig. 14 Relative  $\text{SO}_4^{2-}$  concentrations between days 204 and 318.

$\text{Na}_2\text{S}_2\text{O}_8$  was injected and that the maximum  $\text{SO}_4^{2-}$  concentrations at 19, 22, 25, and 27 m deep were  $1.58 \times 10^4$ ,  $1.86 \times 10^4$ ,  $1.68 \times 10^4$ , and  $1.45 \times 10^4$   $\text{mg L}^{-1}$ , respectively. As the reaction proceeded, the  $\text{SO}_4^{2-}$  concentrations at different depths first decreased and then gradually stabilized. The  $\text{SO}_4^{2-}$  concentration at 19 m decreased most markedly. When  $\text{Na}_2\text{S}_2\text{O}_8$  was activated by NaOH, the  $\text{S}_2\text{O}_8^{2-}$  concentration decreased as the pollutants decomposed and the  $\text{SO}_4^{2-}$  concentration increased. During the chemical oxidation process, the  $\text{SO}_4^{2-}$  concentration negatively correlated with the contaminant concentrations.

For the samples from different depths, the mean  $\text{SO}_4^{2-}$  concentration between days 180 and 200 was used as the initial concentration  $C_0$ , the  $\text{SO}_4^{2-}$  concentration at another time was labeled  $C$ , and the relative  $\text{SO}_4^{2-}$  concentration was expressed as  $C/C_0$ . Regression analysis of the  $\text{SO}_4^{2-}$  concentration over time was performed using SPSS software. The correlation coefficients for the models decreased in the order polynomial model,

power function model, compound model, exponential model, logarithmic model, linear model, meaning the polynomial model fitted the data better than the other models. Even though the polynomial model fitted the data best (had a correlation coefficient  $R$  closest to 1), the serious variations in the high-order model at the end of the data interval meant that the model was not suitable for making predictions. The third-order polynomial fitting model was therefore used to decrease the sensitivity of the model to small variations in the data. The curves are shown in Fig. 14 and the curve fitting equation parameters are shown in Table 7.

According to the correlation coefficient test table,<sup>45</sup> the number of degrees of freedom was 6, and the minimum  $R$  values at the confidence levels of 0.10, 0.05, and 0.01 were 0.62149, 0.70673, and 0.83434, respectively. It can be seen from Table 7 that the third-order fitting correlation coefficients for 19, 22, 25, and 27 m deep were 0.910, 0.973, 0.936, and 0.967, respectively. These  $R$  values were all higher than the minimum  $R$  value. The third-order polynomial equation fitted the data well, and some curves partly predicted variability in the  $\text{SO}_4^{2-}$  concentration. The relative  $\text{SO}_4^{2-}$  concentration in groundwater decreased slowly over time.

High  $\text{SO}_4^{2-}$  concentrations after remediation using ISCO groundwater processes have concerned many researchers. In many ISCO processes, sodium persulfate is activated using an alkali, potassium permanganate, a Fenton reagent, or ozone. All of these oxidizing chemicals give good remediation effects. However, ozone is expensive to produce in practice, potassium permanganate will markedly increase the  $\text{MnO}_4^-$  concentration in groundwater, Fenton reagents will harm the soil environment at very low pH values and add large amounts of ferrous ions, and sodium persulfate activated by an alkali will leave large numbers of  $\text{SO}_4^{2-}$  ions. Our results and the results of many previous studies indicate that the large numbers of  $\text{SO}_4^{2-}$  ions remaining in groundwater after using sodium persulfate activated using an alkali will not be readily degraded because they will be involved in few chemical reactions. However, dilution, recharging, excretion, and biological activities in groundwater will slowly decrease the  $\text{SO}_4^{2-}$  concentration in groundwater decreases. The  $\text{SO}_4^{2-}$  concentration will usually return to the concentration before remediation after 6 months. Using sodium persulfate activated using an alkali will not generally cause long-term adverse effects on the environment and offers more advantages than other oxidizing agents in practice.

## 4. Conclusions

The removal of DNAPLs from groundwater using combined P&T and ISCO processes was studied, and variations in the pH, EC,

Table 7 Curve fitting equation parameters for the relative  $\text{SO}_4^{2-}$  concentrations

| Groundwater depth | Fitting equation: $C/C_0 = -A_1t^3 + A_2t^2 + A_3t + B$ |                    |                     |                    | Correlation coefficient $R$ |
|-------------------|---|--------------------|---------------------|--------------------|-----------------------------|
|                   | $A_1$   | $A_2$              | $A_3$               | $B$                |                             |
| 19 m              | $-3.49 \times 10^6$                                     | $2.54 \times 10^6$ | $-6.16 \times 10^6$ | $4.97 \times 10^6$ | 0.910                       |
| 22 m              | $-3.89 \times 10^6$                                     | $2.83 \times 10^6$ | $-6.85 \times 10^6$ | $5.53 \times 10^6$ | 0.973                       |
| 25 m              | $-3.87 \times 10^6$                                     | $2.82 \times 10^6$ | $-6.91 \times 10^6$ | $5.62 \times 10^6$ | 0.936                       |
| 27 m              | $-4.28 \times 10^6$                                     | $3.13 \times 10^6$ | $-7.63 \times 10^6$ | $6.21 \times 10^6$ | 0.967                       |





DO concentration, and  $\text{SO}_4^{2-}$  concentration were assessed. The practical use of the P&T-ISCO process was simulated. The results are summarized below.

(1) The effect on groundwater remediation of P&T-ISCO using 1.5% sodium persulfate and 0.05% sodium hydroxide was remarkable. As the DNAPL concentrations decreased the pH, EC, and DO concentration tended to become stable and ESM was strongly related to these parameters.

(2) The reaction-diffusion of oxidants and DNAPLs in groundwater was similar to two-dimensional dispersion in a one-dimensional steady flow field. The vertical and horizontal distributions in the aquifers were 0.17 and 0.02 m, respectively. The P&T-ISCO process increased the migration speed through hydraulic driving, which was conducive to diffusion of the chemicals.

(3) During the groundwater restoration process, the  $\text{SO}_4^{2-}$  concentration negatively correlated with the pollutant concentration. A cubic polynomial curve was fitted to the relative  $\text{SO}_4^{2-}$  concentration. The correlation coefficient  $R$  was higher than the critical value, and the curve fitted the data better than the other models that were used. The relative  $\text{SO}_4^{2-}$  concentration decreased slowly over time after the groundwater remediation process was stopped.

## Conflicts of interest

The authors declare there is no conflicts of interest regarding the publication of this paper.

## Acknowledgements

This research was supported by the Science and Technology Major Project of Guangxi (No. AB18281002) and Natural Science Foundation of Guangxi Province (2019GXNSFAA185019).

## Notes and references

- 1 T. Oolman, S. T. Godard, G. A. Pope, M. Jin and K. Kirchner, *Groundwater Monit. Rem.*, 2010, **15**, 125–137.
- 2 D. M. Mackay and J. A. Cherry, *Environ. Sci. Technol.*, 1989, **23**, 630–636.
- 3 K. S. Udell, D. G. Grubb and N. Sitar, *Cent. Eur. J. Public Health*, 1995, **3**, 67–76.
- 4 S. Suthersan, E. Killenbeck, S. Potter, C. Divine and M. LeFrancois, *Ground Water Monit. Rev.*, 2015, **35**, 23–29.
- 5 F. Tatti, M. P. Papini, V. Torretta, G. Mancini, M. R. Boni and P. Viotti, *J. Contam. Hydrol.*, 2019, **222**, 89–100.
- 6 R. W. Wunderlich, J. C. Fountain and R. E. Jackson, *J. Soil Contam.*, 1992, **1**, 361–378.
- 7 R. K. Rothmel, R. W. Peters, E. St. Martin and M. F. DeFlaun, *Environ. Sci. Technol.*, 1998, **32**, 1667–1675.
- 8 A. A. Haluska, C. E. Schaefer, J. Cho, G. M. Lavorgna and M. D. Annable, *J. Contam. Hydrol.*, 2019, 103516, DOI: 10.1016/j.jconhyd.2019.103516.
- 9 R. J. Watts and A. L. Teel, *J. Environ. Eng.*, 2005, **131**, 612–622.
- 10 X. D. Li and F. W. Schwartz, *J. Contam. Hydrol.*, 2004, **68**, 269–287.
- 11 X. D. Li and F. W. Schwartz, *J. Contam. Hydrol.*, 2004, **68**, 39–53.
- 12 A. Tsitonaki, B. Petri, M. Crimi, H. Mosbaek, R. L. Siegrist and P. L. Bjerg, *Crit. Rev. Environ. Sci. Technol.*, 2010, **40**, 55–91.
- 13 J. D. Bryant and J. T. Wilson, *Remediation J.*, 2010, **9**, 13–25.
- 14 R. Baciocchi, L. D'Aprile and I. Innocenti, *J. Cleaner Prod.*, 2014, **77**, 47–55.
- 15 A. K. Boal, C. Rhodes and S. Garcia, *Ground Water Monit. Rev.*, 2015, **35**, 93–100.
- 16 S. H. Liang, C. M. Kao, Y. C. Kuo, K. F. Chen and B. M. Yang, *Water Res.*, 2011, **45**, 2496–2506.
- 17 ITRC, *Overview of Groundwater Remediation Technologies for MTBE and TBA*, The Interstate Technology & Regulatory Council, 2005.
- 18 ITRC, *Technical and Regulatory Guidance for In Situ Chemical Oxidation*, The Interstate Technology & Regulatory Council, 2005.
- 19 A. Long, Y. Lei and H. Zhang, *Prog. Chem.*, 2014, **26**, 898–908.
- 20 C. Liang and C. J. Bruell, *Ind. Eng. Chem. Res.*, 2008, **47**, 2912–2918.
- 21 D. W. Elliott and W. X. Zhang, *Environ. Sci. Technol.*, 2001, **35**, 4922–4926.
- 22 C. Liang and Y. Y. Guo, *Water, Air, Soil Pollut.*, 2012, **223**, 4605–4614.
- 23 J. Kuo, *Practical Design Calculations for Groundwater and Soil Remediation*, CRC Press, 2nd edn, 2014.
- 24 Technical Guideline for Site Soil and Groundwater Sampling of Volatile Organic Compounds HJ 1019-2019.
- 25 Technical guidelines for risk assessment of contaminated sites HJ 25.3-2014.
- 26 Standard for groundwater quality GBT 14848-2017.
- 27 J. H. Smith, D. C. Bomberger and D. L. Haynes, *Environ. Sci. Technol.*, 1980, **14**, 1332–1337.
- 28 S. Pradhan, P. Kumar and I. Mehrotra, *J. Environ. Eng.*, 2016, **142**, 04016034.
- 29 H. U. So, D. Postma, M. L. Vi, T. K. T. Pham, J. Kazmierczak, V. N. Dao, K. Pi, C. B. Koch, H. V. Pham and R. Jakobsen, *Geochim. Cosmochim. Acta*, 2018, **225**, 192–209.
- 30 A. T. Beshia, D. N. Bekele, R. Naidu and S. Chadalavada, *Environ. Technol. Innov.*, 2017, **9**, 303–322.
- 31 D. Oconnor, D. Hou, Y. S. Ok, Y. Song, A. K. Sarmah, X. Li and F. Tack, *J. Controlled Release*, 2018, **283**, 200–213.
- 32 P. Min, *Environ. Eng.*, 2017, **35**, 6–10.
- 33 M. A. Guilbeault, B. L. Parker and J. A. Cherry, *Ground Water*, 2005, **43**, 70–86.
- 34 C. Power, J. I. Gerhard, P. Tsourlos, P. Soupios, K. Simyrdanis and M. Karaoulis, *J. Appl. Geophys.*, 2015, **112**, 1–13.
- 35 P. M. Jeffers and N. L. Wolfe, *Environ. Toxicol. Chem.*, 1996, **15**, 1066–1070.
- 36 H. F. Stroo and C. H. Ward, *Environmental Remediation Technology*, 2010.
- 37 J. L. Liu, W. Lu, F. J. Zhang, X. S. Su and C. Lü, *Environ. Sci.*, 2015, **35**, 2677–2681.
- 38 L. Chen, X. Hu, T. Cai, Y. Yang, R. Zhao, C. Liu, A. Li and C. J. Jiang, *Chem. Eng. J.*, 2019, **369**, 344–352.



- 39 A. Taylor, N. Zrinyi, S. P. Mezyk, J. M. Gleason, L. Mackinnon, A. Przepiora and A. L. Pham, *Water Res.*, 2019, **162**, 78–86.
- 40 A. Santos, J. Fernandez, S. Rodriguez, C. M. Dominguez, M. A. Lominchar, D. Lorenzo and A. Romero, *Sci. Total Environ.*, 2018, **615**, 1070–1077.
- 41 S. H. Liang, C. M. Kao, Y. C. Kuo, K. Chen and B. M. Yang, *Water Res.*, 2011, **45**, 2496–2506.
- 42 X. Yu-Qun, Z. Xue-Chun and W. Ji-Chun, *Groundwater Dynamics*, Geological Publishing House, Beijing, PRC China, 1997.
- 43 Y. Ji, L. Wang, M. Jiang, J. Lu, C. Ferronato and J. Chovelon, *Water Res.*, 2017, **123**, 249–257.
- 44 F. J. Krembs, R. L. Siegrist, M. Crimi, R. Furrer and B. G. Petri, *Ground Water Monitoring Remediation Journal*, 2010, **30**, 42–53.
- 45 M. A. Lominchar, D. Lorenzo, A. Romero and A. Santos, *J. Chem. Technol. Biotechnol.*, 2018, **93**, 1270–1278.

